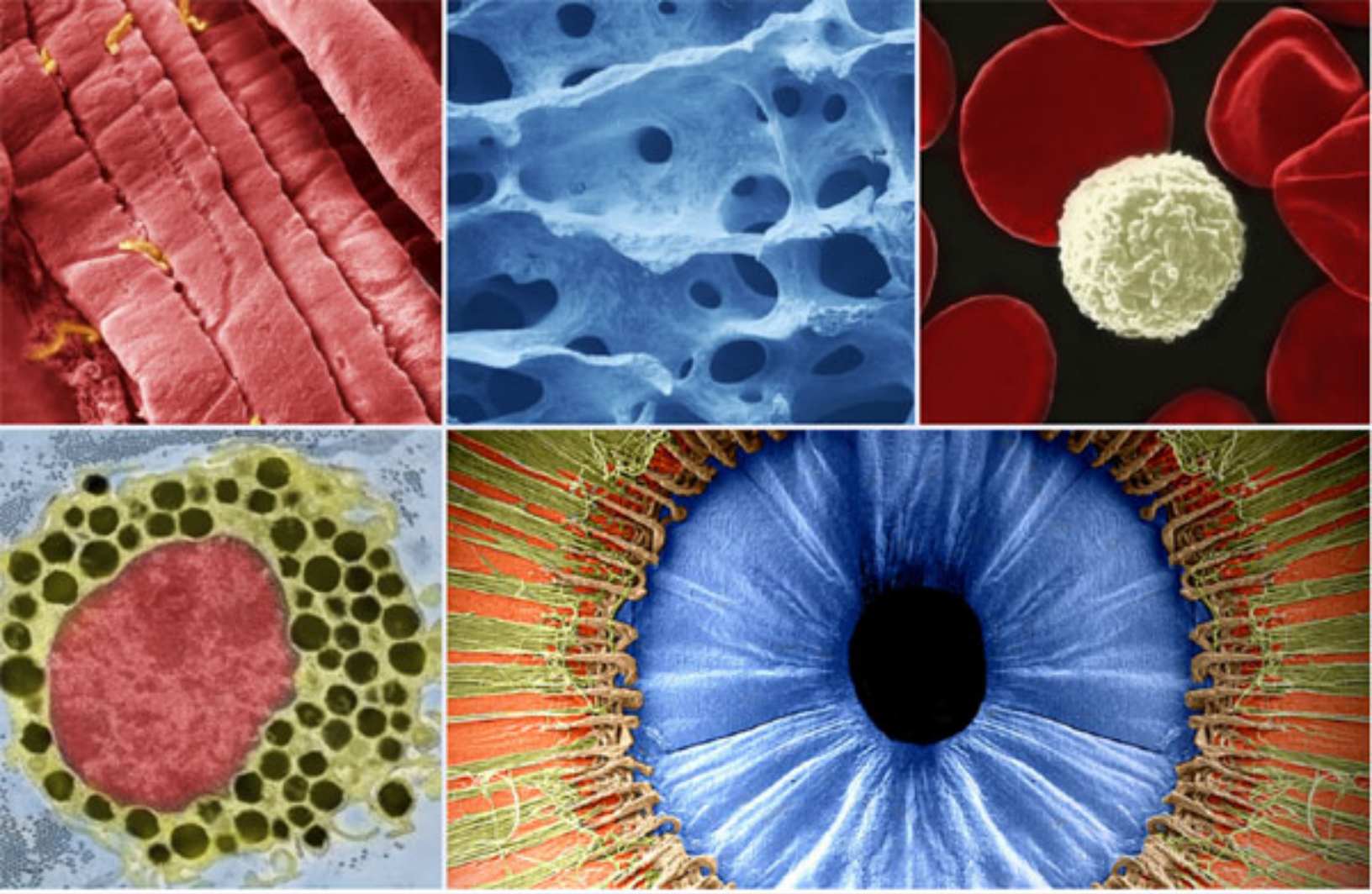

Ultrastructure Atlas of Human Tissues

FRED E. HOSSLER

WILEY Blackwell

ULTRASTRUCTURE ATLAS OF HUMAN TISSUES

Fred E. Hossler, PhD
Professor Emeritus of Biomedical Sciences
J.H. Quillen College of Medicine
East Tennessee State University
Johnson City, Tennessee, USA

WILEY Blackwell

Published by John Wiley & Sons, Inc., Hoboken, New Jersey
Published simultaneously in Canada

Library of Congress Cataloging-in-Publication Data:

Hossler, Fred E., author.
Ultrastructure atlas of human tissues / Fred E. Hossler.
p. ; cm.
Includes bibliographical references and index.
ISBN 978-1-118-28453-7 (cloth)
I. Title.
[DNLM: 1. Histology–Atlases. 2. Tissues–ultrastructure–Atlases. 3. Microscopy, Electron–Atlases. QS 517]
QM557
611′.018–dc23

2013042704

This atlas is dedicated to my parents, Leroy E. and Mildred E. Hossler, who taught me to appreciate the beauty of living things and the value of fine, detailed images of them. Mildred was a well-known water color artist and school teacher in Hamburg, Berks County, Pennsylvania.

CONTENTS

List of Illustrations

FIGURES I-11. and I-14. I-11 Human lymphocytes showing rounded, somewhat indented, and condensed nuclei. ×34 367. I-12 Human neutrophil with extensive nuclear lobation. ×7600. I-13 Human skeletal muscle from the tibialis anterior. Skeletal muscle cells are multinucleated. Seen here are two adjacent muscle cells, each showing a single nucleus along its periphery. ×5106. I-14 Cardiac myocytes from the human atrium. Cardiac myocytes may contain one or two nuclei. The cell at the right center may have two nuclei or, more likely, the tissue section may have been cut along the edge of a single nucleus. ×5000.

FIGURES I-15. to I-18. Clusters of mitochondria from distal tubule cells in the human kidney. M, matrix space; C, cristae. ×45 625, ×61 818, ×81 820, and ×53 500.

FIGURES I-19. to I-20. I-19 Golgi complex in chief cell of human fundus. ×15 000. I-20 Golgi complex in chief cell of human fundus. ×26 700. G, Golgi complex; F, forming face of Golgi; M, maturing face of Golgi; R, rough endoplasmic reticulum; SV, secretory vesicle.

FIGURES I-21. to I-24. I-21 Golgi complex in distal tubule cell of human kidney. ×55 652. I-22 Golgi complex in epithelial cell in human gall bladder. ×7800. I-23 Epithelial cell in human colon. ×11 923. I-24 Epithelial cell in human gall bladder. ×13 000. G, Golgi complex; F, forming face of Golgi complex; M, maturing face of Golgi complex; SV, secretory vesicles; S, smooth endoplasmic reticulum; R, rough endoplasmic reticulum.

FIGURES I-25. to I-26. I-25 Human hepatocyte. I-26 Epithelial cell in human ileum. N, nucleus; R, rough

endoplasmic reticulum; arrows, ribosomes.

FIGURES I-27. to I-30. I-27 to I-29 Rough endoplasmic reticulum in human pancreatic islet cells. ×40 000, ×50 000, and ×40 000. I-30 Rough endoplasmic reticulum in a human hepatocyte. ×24 000. N, nucleus; M, mitochondria; arrows, ribosomes.

FIGURES I-31. to I-32. I-31 Neutrophil within a capillary in the human lung. ×18 139. I-32 Active macrophage in the lamina propria of the human ileum displaying unusually large lysosomes. ×18 750. N, nucleus; arrows, lysosomes.

FIGURES I-33. to I-34. I-33 Human hepatocyte. ×6923. I-34 Fibroblast in the lamina propria of the human colon. ×23 000. N, nucleolus; R, rough endoplasmic reticulum; L, lipid droplets.

FIGURES I-35. to I-38. I-35 Adipose tissue from human dermis. ×77. I-36 Fat cells from human dermis. ×500. I-37 Fat cells from human dermis. ×580. I-38 Cross section of edge of a fat cell from human dermis. ×2500. N, nucleus; F, fat deposit; C, collagen fibrils.

FIGURES I-39. to I-42. I-39 Human liver cell. I-40 Human liver cell. I-41 Keratinocyte from human skin. ×11 600. I-42 Details of cytoplasm of keratinocyte from human skin. ×16 000. G, glycogen; M, mitochrondria; R, rough endoplasmic reticulum; N, nucleus; P, melanin granules; arrow, desmosome.

FIGURES I-43. to I-44. I-43 Apical junction between two epithelial lining cells in the human jejunum. ×39 000. I-44 Apical junction between two epithelial lining cells in the human jejunum. ×92 308. A,

adhering junction; D, desmosomes; M, microvilli; T, tight junction; W. terminal web.

FIGURES I-45. to I-48. I-45 Details of the junctional complex at the apical borders of two epithelial cells in the human jejunum. ×173 077. I-46 A desmosome along the lateral borders of two epithelial cells in the human jejunum. ×133 000. I-47 Two desmosomes joining the adjacent lateral plasma membranes of two epithelial cells in the human jejunum. ×73 000. I-48 Desmosome joining the adjacent lateral plasma membranes of two epithelial cells in the human jejunum. ×74 193. A, adhering junction; D, desmosome; T, tight junction; K, keratin filaments; P, free polysomes; W, terminal web; arrowheads, keratin filaments.

FIGURES I-49. to I-50. I-49 Microvilli on the apical surface of an epithelial cell in the human gall bladder. ×20 100. I-50 Microvilli (brush border) on the surface of the epithelial lining of the human jejunum. M, microvilli; A, actin core of microvilli.

FIGURES I-51. to I-53. I-51 Cross section of microvilli (brush border) on absorptive cells of human jejunum. ×76 023. I-52 Cross section of microvilli (brush border) on absorptive cells of human ileum. ×66 667. I-53 Surface of lining epithelium of human endometrium. ×3000. A, actin core of microvilli; PM, plasma membrane; C, cilia; M, microvilli.

STEREO PAIR I-69. Surface of human mesentery in the region of the ovary/oviduct. Note mesothelial cells.

STEREO PAIR I-70. Details of surfaces of mesothelial cells seen in Stereo Pair I-69.

STEREO PAIR I-71. Details of surfaces of individual mesothelial cells showing abundant microvilli.

FIGURE I-54. Surface of lining epithelium of human trachea. ×4900. C, cilia.

FIGURES I-55. to I-58. I-55 Apical border of bronchial epithelial cell showing microvilli and cilia. ×9032. I-56 Apical surface of bronchial epithelial cell showing microvilli (M), cilia (C), and basal portions of cilia (B). ×31 500. I-57 Apical surface of bronchial epithelial cell showing basal portions of cilia. ×46 095. I-58 Cross sections of cilia on the surface of bronchial epithelial cells showing axoneme cores. ×48 551. M, microvilli; B, basal portion of cilia; C, cilia; MT, microtubules of the axoneme core of cilia; PM, plasma membrane covering cilia.

FIGURES I-59. to I-62. I-59 Cross sections of cilia from the human bronchus. Note “9 + 2” axoneme arrangement of microtubules in cores of cilia. ×89 760. I-60 Cross section of a single cilium from the human bronchus showing details of axoneme core (“9 + 2” arrangement of microtubules). ×247 500. I-61 Cell from human jejunum showing a centriole (arrow) and nuclear pores (arrowheads). ×80 000. I-62 High magnification of the edge of the nucleus of cell from human kidney showing a centriole (arrow) and nuclear pores (arrowheads). Note the ring of nine triplet microtubules making up the centriole. ×206 250. D, dynein side arms of microtubules; MT, microtubules; PM, plasma membranes.

FIGURES I-63. to I-65. I-63 Distal tubule in human kidney. Arrows, cilia. ×3200. I-64 Epithelial lining of Bowman's capsule in human kidney. Arrows, cilia. ×3200. I-65 Epithelial lining of ampulla segment of

FIGURE II-9. Buffy coat from human blood sample. W, white blood cells; R, red blood cells; P, blood platelets. ×9078.

STEREO PAIR II-47. Buffy coat from human blood.

STEREO PAIR II-48. Buffy coat from human blood.

STEREO PAIR II-49. Buffy coat from human blood.

STEREO PAIR II-50. Buffy coat from human blood.

FIGURE II-10. Human blood smear showing sickle cell anemia. ×4020.

FIGURE II-11. Human blood smear showing sickle cell anemia. ×8394.

STEREO PAIR II-51. Sickle cell anemia.

STEREO PAIR II-52. Sickle cell anemia.

STEREO PAIR II-53. Sickle cell anemia.

STEREO PAIR II-54. Sickle cell anemia.

STEREO PAIR II-55. Sickle cell anemia.

FIGURE II-12. Neutrophil in human blood smear. R, red blood cells; arrows, neutrophil specific granules; arrowheads, lysosomal (nonspecific or azure) granules. ×49 600.

FIGURE II-13. Neutrophil in a blood vessel in the wall of the human ureter. E, endothelial cell; R, red blood cell; arrows, neutrophil specific granules; arrowheads; nonspecific (lysosomal, azure) granules. ×74 285.

FIGURE II-14. Neutrophil in a capillary in an alveolar wall of the human lung. E, endothelial cell cytoplasm; P, type I pneumocyte cytoplasm; arrows, neutrophil-specific granules; arrowheads, nonspecific (lysosomal, azure) granules. ×53 823.

FIGURE II-15. Neutrophil in a capillary in an alveoloar wall of the human lung. E, endothelial cell; N, neutrophil; R, red blood cell. ×33 600.

FIGURE II-16. Two neutrophils in a capillary in the lamina propria of the human stomach. N, neutrophil; E; endothelial cell; R; red blood cell. ×11 373.

FIGURE II-17. Eosinophil from the lamina propria of the human ileum. Note the crystals in the centers of the specific eosinophil granules. ×63 600.

FIGURE II-18. Eosinophil from lamina propria of the human small intestine. Note the typical bilobed nucleus and the presence of crystals in the centers of specific eosinophilic granules. Portions of nuclei of two fibrocytes (F) are seen adjacent to the eosinophil.

FIGURE II-19. Eosinophil in lamina propria of human colon. ×24 650. Note crystals in specific eosinophil granules, and note small Golgi complex (G).

FIGURE II-20. Eosinophil in lamina propria of human colon. ×21 760. Note crystals in centers of eosinophil-specific granules.

FIGURE II-21. Eosinophil in lamina propria of human colon. Note crystals in centers of specific eosinophil granules. ×21 265.

FIGURE II-22. Cluster of various size lymphocytes from the lamina propria of the human colon. ×38 142. Note that some common characteristics of lymphocytes include rounded nuclei with some indentations and a high percentage of heterochromatin, and numerous cell surface pseudopodia. Arrows; mitochondria.

FIGURE II-23. Cluster of lymphocytes from the lamina propria of the human colon. ×38 152. Note typical rounded nuclei with a high level of heterochromatin and some indentations, and note cell surface pseudopodia. C, collagen fibrils in the lamina propria.

FIGURE II-24. Two lymphocytes in the lamina propria of the human colon. ×67 936. C, collagen fibrils in the lamina propria; arrows, mitochondria.

FIGURES II-25. and II-26. II-25 Two lymphocytes from the lamina propria of the human colon. ×44 000. II-26 Lymphocyte within a capillary in the wall of the human atrium. ×13 200. E, endothelial cell; M, mitochondria; N, nucleoli; arrows, rough endoplasmic reticulum.

FIGURE II-27. Lymphocyte in lamina propria of human colon. ~×90 000.

FIGURE II-28. Large lymphocyte from lamina propria of human colon. The increase in amount of cytoplasm and cytoplasmic organelles occurs with lymphocyte activation for antibody synthesis. G, Golgi complex; M, mitochondria; arrows, rough endoplasmic reticulum. ~×60 000.

FIGURES II-29. and II-30. II-29 Lymphocyte from lamina propria of human colon ~×26 000. II-30 Lymphocyte from lamina propria of human colon. ~×26 000. N, nucleolus; arrow, Golgi complex; arrowheads, mitochondria.

FIGURE II-31. Diapedesis of a lymphocyte through the endothelium of a capillary in the lamina propria of the human colon. ×3750. E, endothelial cell; L, lymphocyte; R, red blood cells; F, fibrocytes in lamina propria.

FIGURE II-32. Diapedesis of a lymphocyte through a vessel wall. ×16 400. E, endothelial cell cytoplasm; L, lymphocyte.

FIGURE II-33. White blood cell (possible lymphocyte) and several red blood cells. ×12 325.

FIGURE II-34. Macrophage in the lamina propria of the human colon. Note abundant phagocytic vesicles. A portion of a second macrophage is seen at the bottom of the image. ×29 000.

FIGURE II-35. Two “dust cells” (macrophages) in an alveolar space in the human lung. Note abundant cytoplasmic phagocytic vesicles in these active phagocytes. ×25 540.

FIGURE II-36. The inside lining of an alveolus in the human lung showing “dust cells” (macrophages, arrows), type II pneumocytes (arrowheads), and an alveolar pore (P). Note that the macrophages are free, wandering cells, while the pneumocyte type II cells are in a fixed position in the alveolar wall. ×760.

FIGURE II-37. Inside lining of an alveolus in the human lung. Note wandering macrophages (dust cells, M), pneumocyte type II cells (II), a few free red blood cells (R) resulting from tissue preparation, and the borders (arrows) of flattened pneumocyte type I cells which cover the alveolar surface. The “rounded ridges” that are seen along the alveolar wall are formed by a network of capillaries lying just beneath the flattened type I pneumocytes. ×2300.

FIGURE II-38. Human blood smear showing a cluster of platelets (P) and a few red blood cells (R). ×11 600.

FIGURE II-39. Neutrophil with a single, disc-shaped blood platelet (P) above it. In the neutrophil, note the

multilobed nucleus, the central Golgi complex (G), and the granule-rich cytoplasm. Most of the large granules are nonspecific (lysosomal) granules, and most of the smaller granules are neutrophil-specific granules. Note also the granule-rich cytoplasm of the platelet. ×64 000.

FIGURE II-40. Blood platelet at the edge of a sinusoid in the human liver. Note the granular cytoplasm and the peripheral ring of microtubules (arrows) in the platelet. E, endothelial cell; D, space of Disse; H, hepatocyte; M, mitochondria; arrowheads, rough endoplasmic reticulum.

FIGURE II-41. (a) Fenestrated capillary from the human ileum containing a cluster of blood platelets. Note the granule-rich cytoplasm of the platelets. (b) Higher magnification of several of the blood platelets in (a). E; endothelial cell; P, blood platelets; arrows, peripheral rings of supporting microtubules. (a) ×39 000 and (b) ×117 000.

FIGURE II-42. Human blood clot showing clumped red blood cells (R) and fibrin fibers (arrows). Platelets are not visible. ×2250.

FIGURE II-43. Human blood clot showing clumped red blood cells (R), a few white blood cells (W), and fibrin filaments (arrows). ×2250.

Chapter 3

FIGURE III-1. Collagen type I fibrils in loose connective tissue associated with a peripheral nerve. Note cross banding on the individual fibrils. ×67 500.

FIGURE III-2. Collagen type I fibrils from loose connective tissue. Note cross banding. Several fibrils are seen in cross section in the upper right corner of the image. ~×135 000.

FIGURE III-3. Collagen type I fibrils from loose connective tissue associated with the human ureter. Note banding pattern on fibrils. ~×81 000.

FIGURE III-4. Cross sections of collagen type I fibrils in loose connective tissue near a peripheral nerve. ×115 000.

FIGURE III-5. Collagen fibrils from loose connective tissue cut in cross section. These are probably collagen types I and III. ~×162 000.

FIGURE III-6. Bundle of collagen type I fibers in dense irregular connective tissue of the human dermis. ×3810.

FIGURE III-7. Bundles of collagen type I fibers in dense irregular connective tissue in the human dermis. ×5368.

FIGURE III-8. (a) and (b) Collagen I fibers in dense irregular connective tissue from the human dermis. (a) ×1242 and (b) ×800.

FIGURE III-9. Collagen type I fibrils in dense irregular connective tissue in the human dermis. Note the cross banding on the fibrils. ×137 931.

FIGURE III-10. (a) and (b) Collagen type I fibrils from human flexor carpi radialis tendon—a longitudinal view showing cross banding. (a) ×115 938 and (b) ×126 373.

FIGURE III-11. Details of cross banding on collagen I fibrils in dense regular connective tissue in the human flexor carpi radialis tendon. ×127 753.

FIGURE III-12. (a) and (b) Cross banding of collagen I fibrils in dense regular connective tissue of human flexor carpi radialis tendon. The banding pattern results from the precise parallel longitudinal

orientation of collagen molecules in the fibrils. Collagen molecules overlap each other by about a quarter of their length, leaving a small gap between the amino terminus of one protein molecule and the carboxy terminus of the next protein molecule. The repeating band pattern (see arrows) is about 68 nm in width. (a) ×125 000 and (b) ×233 215.

FIGURE III-13. Loose connective tissue in the lamina propria of the human liver. Portions of three fibroblasts (F) are seen, surrounded by bundles of collagen cut longitudinally (LS) and in cross section (XS). The fibroblasts are in a synthetically inactive state as indicated by the small amount of rough endoplasmic reticulum (arrows) in their cytoplasm. Portions of epithelial cells lining a bile duct (B) are seen in the upper right corner of the figure. Arrowheads, basement membrane of the bile duct. ~×39 000.

FIGURE III-14. Fibroblast in loose connective tissue of the lamina propria of the human colon. Note that connective tissue at this site is composed primarily of ground substance with a few scattered collagen fibers. Small amounts of rough endoplasmic reticulum (arrows) are seen in the cytoplasm of this relatively inactive fibroblast. N, nucleolus. ×38 780.

FIGURE III-15. Connective tissue associated with the capsule of the human gall bladder. Clusters of collagen fibers (C) and masses of ground substance (G) are seen surrounding a small lymphocyte (L) and a fibroblast (F). Small amounts of rough endoplasmic reticulum (arrows) as well as a small lipid droplet (arrowhead) can be seen in the cytoplasm of the fibrocyte. N, nucleoli. ×6603.

FIGURE III-16. Loose connective tissue in the lamina propria of the human colon. Several spindle-shaped fibroblasts (F) are seen in loose connective tissue matrix located between two capillaries (C). Note collagen fiber bundles (B), ground substance (G), endothelial cells (E), and red blood cells (R). ×7500.

FIGURE III-17. Fibroblast in dense irregular connective tissue of the human dermis. The light background matrix consists mostly of collagen type I fibers and ground substance. ×10 000.

FIGURE III-18. Dense irregular connective tissue in the capsule of the human spleen. C, collagen fibers; F, processes of attenuated fibroblasts. ×21 818.

FIGURE III-19. Dense irregular connective tissue in the capsule of the human spleen. C, collagen fibers; F, processes of attenuated fibroblasts. ×28 676.

FIGURE III-20. (a), (b), (c), and (d) Fibroblasts in the dense regular connective tissue of the human flexor carpi radialis tendon. Note that the fibroblasts are very attenuated and stellate and are essentially in an inactive state. They are there primarily to maintain the connective tissue matrix as needed. The matrix consists primarily of collagen I and ground substance. (a) ×5878, (b) ×10 345, (c) ×10 404, and (d) ×4091.

FIGURE III-21. (a), (b), (c), and (d). Fibroblasts in dense regular connective tissue of the human flexor carpi radialis tendon. The matrices here show primarily collagen type I fibrils in cross section (arrows). (a) ×10 510, (b) ×9047, (c) ×16 667, and (d) ×16 000.

FIGURE III-22. (a) and (b) Fibroblasts in dense regular connective tissue from the human flexor carpi radialis tendon. Note collagen fibrils in long section (a) and in cross section (b). In (c) and (d), collagen fibrils in cross section in human flexor carpi radialis tendon. The thick fibrils (C) are likely collagen type I and the thin fibrils (arrows) may be collagen type III. (a) ×22 556, (b) ×14 000, (c) ×40 000, and (d) ×62 500.

FIGURE III-23. Adipose tissue associated with the surface of the human gall bladder. The mass of adipocytes is supported by a network of collagen fibers. ×143.

FIGURE III-24. Adipose tissue. Clusters of adipocytes are supported by a network of collagen fibers. ×230.

FIGURE III-25. Adipose tissue mass from the human lower leg adjacent to the gastrocnemius tendon. ×86.

FIGURE III-26. Adipose tissue. Adipocyte cells are covered by a network of thick and delicate collagen fibers. The thick fibers are likely collagen type I, and some of the very delicate fibers may be collagen III. ×430.

FIGURE III-27. Adipose tissue from human hypodermis in pubic region. ×342.

FIGURE III-28. Human adipocytes supported by collagen fibers. ×1200.

FIGURE III-29. Adipocytes from adipose tissue in hypodermis of human upper leg. The very delicate connective tissue fibers on the adipocyte surfaces are composed primarily of collagen III. ×1353.

FIGURE III-30. Human adipocytes. The large collagen fibers (C) in the center and lower left of the image are likely collagen I, and the delicate fibers (arrows) barely visible on the adipocyte cell surfaces are likely collagen III. ×1135.

FIGURE III-31. Adipocytes from connective tissue associated with the mesentery near the human gall bladder. The larger fibers (C) near the top of the image are likely collagen I, whereas the delicate fibers adhering to the cell surfaces (arrows) are likely collagen III. ×1025.

FIGURE III-32. Human adipocytes. ×848.

FIGURE III-33. (a) and (b) Adipocytes from human hypodermis. Fig. III-33b is a cross section of the cell surface of an adipocyte showing its nucleus within a thin rim of cytoplasm. ×1140.

FIGURE III-34. Adipocytes and collagen fibers in human adipose tissue. ×2050.

FIGURE III-35. High magnification of connective tissue fibers on the surface of a human adipocyte. The larger fibers seen on the cell surface are likely collagen I, and the finer fibers are likely collagen III. ×8632.

FIGURE III-36. Connective tissue fibers on the surface of an adipocyte in human connective tissue. The fibers represent several types of collagen. ~×9000.

FIGURE III-37. Connective tissue fibers on the surface of a human adipocyte. The fibers represent various types of collagen. ~×13 000.

FIGURE III-38. High magnification image of the surface of an adipocyte from human hypodermis

showing details of collagen fibers. The large fibers are likely collagen I (CI) and the small fibers are likely collagen III (CIII). ×11 785.

FIGURE III-39. High magnification of collagen fibers on the surface of an adipocyte from human hypodermis. The large fibers likely are collagen I (CI), and the small fibers are likely collagen III (CIII). ×8000.

STEREO PAIR III-80. Adipocytes from human dermis.

STEREO PAIR III-81. Adipocytes from human dermis.

FIGURE III-40. Two mast cells (M) in the lamina propria of the human colon. Note the distinct cytoplasmic granules and the numerous surface microvilli, characteristic of mast cells. The edge of a capillary (C) is seen at the lower right corner of the image and a segment of a peripheral nerve (N) is present at the top of the image. The thin strands (arrows) seen within the connective tissue matrix are cytoplasmic processes of flattened fibroblasts. B, collagen bundles; G, ground substance; E, endothelial cell. ×5614.

FIGURE III-41. Mast cell in the lamina propria of the human stomach. Note the prominent cytoplasmic granules. ~×17 096.

FIGURE III-42. (a) Mast cell in the lamina propria of the human stomach. (b) Mast cell in the lamina propria of the human colon. Note the prominent cytoplasmic granules of the mast cells in each image. G, Golgi complex. (a) ~×11 790 and (b) ~×15 454.

FIGURE III-43. (a) and (b) Mast cells in the lamina propria of the human colon. Note the abundant

cytoplasmic granules and surface microvilli. (a) ~×15 540 and (b) ~×13 700.

FIGURE III-44. (a) and (b) Mast cells in the lamina propria of the human ileum. (c) Mast cell in the interlobular connective tissue of the human liver. (d) Mast cell in the lamina propria of the human stomach. ×6452. C, collagen fibers; G, ground substance.

FIGURE III-45. Mast cell in the lamina propria of the human ileum. Note the prominent granules in the cytoplasm and the abundant microvilli on the cell surface. C, collagen fibers; G, ground substance. ~×60 923.

FIGURE III-46. (a) and (b) Plasma cells and one mast cell (M) in the lamina propria of the human colon. Note characteristic chromatin pattern and rough endoplasmic reticulum-rich cytoplasm in all plasma cells. (a) ×7411 and (b) ×6382.

FIGURE III-47. This plasma cell in the lamina propria of the human colon displays all the classic characteristics of this cell type—an eccentric nucleus with a “spoke wheel” heterochromatin pattern, a perinuclear Golgi “halo” region in the cytoplasm, and a cytoplasm rich in profiles of rough endoplasmic reticulum. Arrows, mitochondria; arrowhead, centriole. ~×25 000.

FIGURE III-48. (a) Plasma cell in the lamina propria of the human jejunum. **(**b) Plasma cell in the lamina propria of the human ileum. In each case note “spoke wheel” pattern of heterochromatin and rough endoplasmic reticulum-rich cytoplasm. Arrows, mitochondria.

FIGURE III-49. (a), (b), and (c) Plasma cells in the lamina propria of the human colon. Note the eccentric nuclei and rough endoplasmic reticulum-rich cytoplasm in each cell. In (a) and (b), note the very distinct “spoke wheel” pattern of the heterochromatin. N, nucleolus. The magnification of (a) is about 17 647.

FIGURE III-50. (a) to (d) Plasma cells in the lamina propria of the human ileum. Arrow, centriole; arrow heads, mitochondria. Image magnifications are about 10 000.

FIGURE III-51. Plasma cell cluster in the lamina propria of the human colon. Note typical “spoke wheel” chromatin pattern and rough endoplasmic reticulum-rich cytoplasm in these cells. N, nucleolus; arrow, centriole. ×10 000.

FIGURE III-52. Dense regular connective tissue in the cross section of a tendon from a human wrist surgery. ×58.

FIGURE III-53. Dense regular connective tissue in the cross section of a tendon from a human wrist surgery. ×118.

FIGURE III-54. (a), (b), and (c) Collagen type I fibers (cross section in (a) and long sections in (b) and (c) in dense regular connective tissue in tendons from a human wrist surgery. (a) ×1639, (b) ×850, and (c) ×336.

FIGURE III-55. Collagen type I fibers from dense regular connective tissue in a section of tendon from a human wrist surgery. ×1034.

FIGURE III-56. (a) and (b) Collagen type I fibers from the human flexor carpi radialis tendon. (a) ×752 and (b) ×1540.

FIGURE III-57. (a) and (b) Collagen type I fibers in dense regular connective tissue from the human flexor carpi radialis tendon. (a) ×4069 and (b) ×5000.

FIGURE III-58. Collagen type I fibers from a tangentially sectioned human flexor carpi radialis tendon. ×2600.

STEREO PAIR III-82. Cross section of human gastrocnemius tendon.

STEREO PAIR III-83. Human gastrocnemius tendon.

STEREO PAIR III-84. Human gastrocnemius tendon.

STEREO PAIR III-85. Human gastrocnemius tendon.

STEREO PAIR III-86. Human gastrocnemius tendon.

STEREO PAIR III-87. Human flexor carpi radialis tendon.

STEREO PAIR III-88. Human flexor carpi radialis tendon.

STEREO PAIR III-89. Human flexor carpi radialis tendon (lateral view).

STEREO PAIR III-90. Human flexor carpi radialis tendon (lateral view).

STEREO PAIR III-91. Collagen I fibers in human gastrocnemius tendon (tangential section).

STEREO PAIR III-92. Collagen I fibers in human gastrocnemius tendon (tangential section).

FIGURE III-59. Hyaline cartilage plate from human trachea, split open. P, perichondrium. ×59.

FIGURE III-60. Interior of hyaline cartilage plate from human trachea. P, perichondrium. ×202.

FIGURE III-61. (a) and (b) Interior of hyaline cartilage plates from human trachea. Arrows, chondrocytes in lacunae; arrowheads, lacunae. (a) ×168 and (b) ×340.

FIGURE III-62. Interior of hyaline cartilage plate from human trachea. Fibrous appearance of matrix (M) is due to collagen type II fibers embedded in ground substance. C, chondrocytes in lacunae; L, lacunae. ×509.

FIGURE III-63. Details of hyaline cartilage from human trachea. Note fibrous appearance of matrix (M) due to the presence of collagen type II fibers embedded in ground substance. C, chondrocytes in lacunae. ×991.

FIGURE III-64. Two chondrocytes embedded in hyaline cartilage matrix from the human trachea. ×8450.

FIGURE III-65. Chondrocytes in the matrix of hyaline cartilage from the human trachea. Because of their proximity to each other, these three cells are likely members of an isogenous group. The matrix immediately surrounding each cell is slightly different in appearance from the rest of the matrix, and was thus likely newly synthesized by these cells. ×6913.

FIGURE III-66. Fibrocartilage from human bunion surgery. The fibrous appearance of the cartilage matrix (M) is due to the presence of collagen type I fibers embedded in ground substance. Arrows, chondrocytes in lacunae. ×245.

FIGURE III-67. Fibrocartilage from human bunion surgery. Chondrocytes were extracted from the two